HHS Public Access

Author manuscript

Cell Rep. Author manuscript; available in PMC 2017 November 01.

Published in final edited form as:

Cell Rep. 2017 October 24; 21(4): 867–877. doi:10.1016/j.celrep.2017.10.004.

Columnar-Intrinsic Cues Shape Premotor Input Specificity in Locomotor Circuits

Myungin Baek[1], **Chiara Pivetta**[2,3], **Jeh-Ping Liu**[4], **Silvia Arber**[2,3], and **Jeremy S. Dasen**[1,*]

[1]Neuroscience Institute, Department of Neuroscience and Physiology, NYU School of Medicine, New York, NY 10016, USA [2]Biozentrum, Department of Cell Biology, University of Basel, Klingelbergstrasse 70, 4056 Basel, Switzerland [3]Friedrich Miescher Institute for Biomedical Research, Maulbeerstrasse 66, 4058 Basel, Switzerland [4]Department of Neuroscience, University of Virginia School of Medicine, Charlottesville, VA 22908, USA

Summary

Control of movement relies on the ability of circuits within the spinal cord to establish connections with specific subtypes of motor neuron (MNs). Although the pattern of output from locomotor networks can be influenced by MN position and identity, whether MNs exert an instructive role in shaping synaptic specificity within the spinal cord is unclear. We show Hox transcription factor-dependent programs in MNs are essential to establish the central pattern of connectivity within the ventral spinal cord. Transformation of axially-projecting MNs to a limb-level lateral motor column (LMC) fate, through mutation of the *Hoxc9* gene, causes the central afferents of limb proprioceptive sensory neurons to target MNs connected to functionally inappropriate muscles. MN columnar identity also determines the pattern and distribution of inputs from multiple classes of premotor interneurons, indicating that MNs broadly influence circuit connectivity. These findings indicate that MN-intrinsic programs contribute to the initial architecture of locomotor circuits.

Graphical abstract

*Lead contact: jeremy.dasen@nyumc.org

Author Contributions

MB and JD devised the project, designed the experiments, and wrote the paper. CP and SA provided viral reagents, and analyzed transsynaptic tracing. JPL generated the *Hoxc9* conditional allele and performed preliminary analysis of mutants. All authors read the paper.

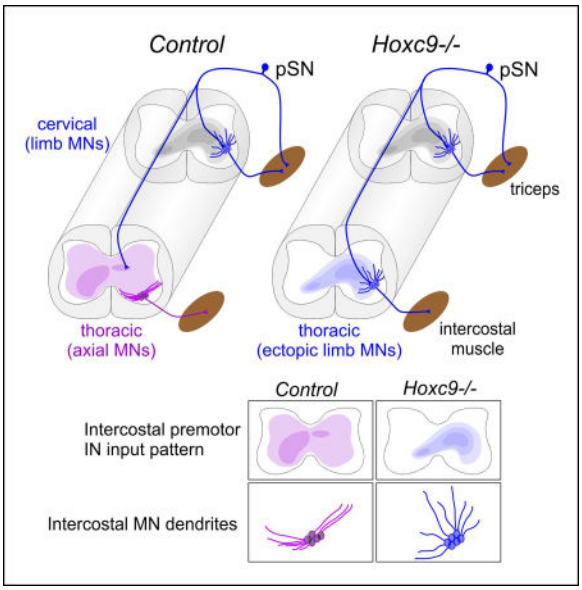

Introduction

Circuits within the vertebrate brainstem and spinal cord are capable of generating motor output that reflect the rhythm and pattern of muscle activation deployed during basic motor behaviors including walking and breathing (Goulding, 2009; Grillner, 2006). The assembly of motor circuits relies on the specificity of synaptic connections established between motor neurons, proprioceptive sensory neurons, and spinal interneurons during embryonic development (Arber, 2012; Catela et al., 2015). In the networks controlling locomotion, limb muscle activation sequences are orchestrated by central pattern generators (CPGs) composed of several classes of excitatory and inhibitory spinal interneurons (Goulding, 2009). The activities of locomotor CPGs can be adjusted by muscle-derived sensory feedback transmitted by proprioceptive sensory neurons (pSNs), which synapse with local interneuron and MN subtypes (Rossignol et al., 2006). Although circuits comprised of CPGs, MNs, and pSNs are essential to coordinate locomotor output, the mechanisms through which they assemble into functional networks are poorly understood.

A critical step in locomotor circuit assembly is the selective targeting of limb muscles by spinal MNs. A network of Hox transcription factors is required for the specification of limb-innervating lateral motor column (LMC) neurons, as well as its resident MN pools targeting individual muscles (Jessell et al., 2011; Philippidou and Dasen, 2013). While the specification of MNs by *Hox* genes is critical for muscle target specificity, the extent to which MN identity contributes to central connectivity in motor networks is unclear (Dasen, 2016). Studies investigating the assembly of spinal reflex circuits have led to differing conclusions about the relative importance of MNs. Evidence supporting a MN-independent program has emerged through analysis of connections between pSNs and MNs under conditions where motor pool specification programs are lost. Mutation in the Hox-dependent transcription factor *Foxp1* strips LMC neurons of MN pool-specific programs, and motor axons select muscle targets in a random manner (Dasen et al., 2008; Rousso et al., 2008).

Nevertheless, pSNs project to the appropriate dorsoventral position within the ventral spinal cord and synapse with MNs, irrespective of which limb muscle is targeted (Surmeli et al., 2011).

In contrast, analyses of sensory-motor connectivity under conditions where only a subset of MN pools are affected provide evidence that target-induced molecular recognition programs can direct specificity in reflex circuits. Expression of the transcription factor *Pea3* is induced by limb-derived neurotrophins in MNs, and in the absence of *Pea3*, pSNs target inappropriate MN subtypes (Livet et al., 2002; Vrieseling and Arber, 2006). Pea3 controls expression of the guidance receptor ligand *Sema3e*, and while MN position is unaffected in *Sema3e* mutants, pSNs target inappropriate MNs (Pecho-Vrieseling et al., 2009). Although target-induced expression of guidance determinants is one strategy for controlling specificity in reflex circuits, they appear to operate in only a limited number of MN pools. Given that Hox proteins govern MN diversification independent of peripheral signals (Dasen et al., 2005), key aspects of sensory-motor connectivity could be controlled through MN-intrinsic pathways.

Beyond spinal reflex circuits, evidence suggests that MNs may play broader roles in determining connectivity with multiple neuronal populations, including the diverse classes of premotor interneurons that comprise CPG networks. Although loss of an LMC identity in *Foxp1* mutants has no apparent effect on the central targeting of pSN axons, the pattern of output from locomotor CPGs is disrupted. In *Foxp1* mutants there is a loss of extensor-like bursting pattern, suggesting that molecular programs acting within LMC neurons contribute to connectivity between spinal interneurons and specific MN subtypes (Hinckley et al., 2015; Machado et al., 2015). In addition, MN columns targeting limb and axial muscle have been shown to be engaged by distinct populations of premotor interneurons (Goetz et al., 2015). While these studies suggest MNs contribute to locomotor network activity, whether MNs influence connectivity with spinal interneurons has not been investigated.

In this study, we assessed whether MN identity and organization determines the specificity of inputs from premotor neurons. We show that transformation of MNs targeting hypaxial muscle to a limb-level LMC fate causes marked changes in the central projections and target specificity of proprioceptive sensory neurons. Conversion of axial MNs to an LMC fate also alters the distribution of inputs from spinal premotor interneurons, indicating a prominent role for MNs in motor circuit assembly.

Results

Hoxc9 Activity Shapes the Central Pattern of Cervical Sensory Neuron Projections

To determine whether MN identity contributes to the specificity of connections within the ventral spinal cord, we examined the formation of sensory-motor reflex circuits under conditions where MN organization has been genetically altered. We first traced the central projections of sensory neuron (SN) afferents along the rostrocaudal axis in controls by injecting the lipophilic dye DiI into dorsal root ganglia (DRGs) of postnatal day (P) 0–P1 mice. Cervical (C) DRGs contain pSNs targeting predominantly forelimb muscles, whereas thoracic (T) pSNs target dorsal epaxial and ventral hypaxial muscles. This analysis revealed

that the projections of cervical and thoracic SNs to MNs were restricted to segments where the corresponding columnar subtypes are present, whereas central branches at other segmental levels terminate in the intermediate spinal cord. Anterograde tracing from DRGs C7 labeled sensory afferents projecting to the ventral spinal cord between segments C5–T1, where the cell bodies of LMC neurons reside (Figure 1A). In contrast, at thoracic segments (T2–T5) cervical SN collaterals terminated in the intermediate spinal cord (Figure 1A). Similarly, tracing from thoracic DRGs labeled sensory neurons projecting to thoracic MNs, but were restricted to intermediate spinal cord at cervical levels (Figure 1A). These data indicate that the central afferents of cervical SNs target LMC neurons, while thoracic SNs target MNs in thoracic segments.

To explore whether MN identity influences the central projection of SNs, we traced afferents under conditions where the columnar fate of MNs has been transformed. The *Hoxc9* gene is expressed at thoracic levels and is essential for the organization of MN subtypes along the rostrocaudal axis. In *Hoxc9* mutants thoracic hypaxial motor column (HMC) and preganglionic motor column (PGC) neurons are converted to an LMC fate, in part, due to the derepression of cervical *Hox4–Hox8* genes and *Foxp1* at thoracic levels (Jung et al., 2010). To determine if the ventral termination zones of SN afferents are influenced by MN columnar identity, we examined sensory projections in global *Hoxc9* mutants. Injection of DiI into DRG C7 in *Hoxc9* mutants labeled sensory axons extending to the ventrolateral thoracic spinal cord, where ectopic LMC neurons reside (Figure 1B). Sensory neurons originating from C7 targeted the ventrolateral spinal cord over multiple segments in *Hoxc9* mutants, extending from T2 to T5 (Figure 1B–D). Injection of DiI into DRGs C5, C6, and C8 in *Hoxc9* mutants also labeled sensory afferents extending to MNs at thoracic levels, revealing loss of *Hoxc9* has a widespread effect on the central targeting of forelimb-level sensory neurons (Figure S1A).

In principle, the extension of limb SNs to thoracic MNs could compete with the ability of thoracic SNs to target MNs. We therefore assessed the consequences of the presence of limb sensory axons on the projection of thoracic sensory afferents to MNs. Thoracic SNs were traced by DiA injection into DRG T3, while cervical sensory afferents were traced in parallel by injection of DiI into DRG C7. This analysis revealed that both cervical and thoracic SNs project afferents into the region occupied by ectopic LMC neurons (Figure 1E). These results indicate that in the absence of *Hoxc9*, limb-level SNs extend axons toward ectopic LMC neurons, but do not preclude the ability of thoracic SNs to target the ventral spinal cord (Figure 1F).

Supernumerary axonal projections are often generated during early stages of neuronal development, and are subsequently removed as circuits mature (Luo and O'Leary, 2005). The extension of limb SNs to thoracic MNs in *Hoxc9* mutants might reflect the maintenance of projections that existed at earlier stages. We therefore assessed whether limb SNs initially project collaterals to thoracic MNs. DiI was injected into DRG C8 between e12.5 and e18.5 and the central projections of SNs were analyzed in cervical and thoracic segments. In control mice, SNs originating from C8 enter the spinal cord by e13.5, approach the ventral spinal cord at e14.5, and target cervical MNs by e15.5 (Figure S1B). Although cervical sensory afferents extend to thoracic segments, they did not project to thoracic MNs at any

stage in control animals. In *Hoxc9* mutants, C8-derived SNs extend to thoracic MNs over the same time window as cervical LMC neurons, beginning at e15.5 (Figure S1B). The projection of limb SNs to thoracic MNs in *Hoxc9* mutants therefore does not result from the maintenance of projections that existed earlier.

The *Hoxc9* gene is expressed by interneurons and non-neuronal tissues, raising the question of whether the observed phenotypes are specifically due to the transformation of MN columnar identities. To address this, we selectively removed *Hoxc9* from the ventral spinal cord. We generated a floxed *Hoxc9* allele and crossed this line with *Olig2::Cre* mice, in which Cre is expressed by MN progenitors, and transiently by V2 and V3 interneuron precursors (Chen et al., 2011; Dessaud et al., 2007) (Figure S2A–C). In *Hoxc9* conditional mutants (*Hoxc9*^{CM} mice), *Hoxc9* is extinguished from MNs and *Hox* genes normally restricted to cervical levels are derepressed in thoracic MNs, similar to global *Hoxc9* mutants (Figure S2D,E) (Jung et al., 2010). In addition, thoracic MN columnar subtypes (PGC and HMC neurons) were depleted in *Hoxc9*^{CM} mice, and LMC neurons (defined by Foxp1 and Raldh2 expression) were ectopically generated in segments T1–T5 (Figure S2F,G). Ectopic LMC neurons also expressed the transcription factors Pea3 and Scip, markers for MN pools residing in caudal cervical segments (Figure S2E,G).

We traced sensory afferent projections from cervical DRG in *Hoxc9*^{CM} mice by DiI injection into DRG C7. Similar to *Hoxc9* global mutants, cervical SNs projected afferents into the ventral thoracic spinal cord in *Hoxc9*^{CM} mice (Figure 2A). As with global *Hoxc9* mutants, C7-derived sensory projections were directed to the lateral region of the ventral spinal cord, where ectopic LMC neurons reside (Figure 2B,C). These observations indicate that the changes in sensory projections in *Hoxc9* mutants are specifically due to neuronal transformations in the ventral spinal cord.

Limb pSNs Establish Functional Synapses with Ectopic LMC Neurons in *Hoxc9* Mutants

Tracer injection into DRG indiscriminately labels multiple classes of SNs, raising the question of whether the ectopic projections in *Hoxc9* mutants derive from proprioceptive SNs, and whether they establish functional connections with MNs. We used muscle-specific tracer injections to assess whether synapses are established between limb pSNs and thoracic LMC neurons in *Hoxc9* mutants. Forelimb pSNs were traced by injection of cholera toxin subunit B (CTB) into the triceps muscle at P3 and synapses with MNs were examined at P5. Boutons on MNs were visualized through colocalization of CTB with vesicular glutamate transporter 1 (vGluT1), which labels the terminals of type Ia pSN afferents. In control mice, vGluT1^{+}; CTB^{+} terminals of triceps pSNs localized to the dorsomedial thoracic spinal cord, similar to the restriction observed in DiI tracing (Figure 3A,E). By contrast, in global and conditional *Hoxc9* mutants vGluT1^{+}; CTB^{+} triceps pSNs terminals localized to the ventrolateral thoracic spinal cord where ectopic LMC MNs are located (Figure 3A,E). In global *Hoxc9* mutants, vGluT1^{+}; CTB^{+} terminals of triceps pSNs were observed on the soma of thoracic MNs, but were not observed in control animals (225.9± 54.44 [mean ±SEM] synapses/30μm section in n=5 *Hoxc9*$^{-/-}$ mice, versus 0±0 in n=5 control mice, **p=0.0032) (Figure 3B,C). Similarly, tracing from the triceps muscle in *Hoxc9*^{CM} mice labeled vGluT1^{+} terminals that extended ventrally and established synapses with MNs

(45.48±11.09 [mean±SEM] synapses/30μm section in n=8 *Hoxc9*^{CM} mice, versus 0±0 in n=6 controls, **p= 0.0043) (Figure 3F,G). Ectopic synapses on thoracic MNs were also observed after tracer injections into biceps, distal flexor, and distal extensor limb muscles in *Hoxc9*^{CM} mice (Figure S3A). These results indicate that limb pSNs establish synapses with ectopic LMC neurons in *Hoxc9* mutants.

Because the observed connections between limb pSNs and ectopic LMC neurons could be attributed to a rerouting of thoracic MNs to limb muscle, we assessed the position of the triceps MN pool, as well as the peripheral target specificity of supernumerary LMC neurons in *Hoxc9* mutants. Retrograde tracing from triceps in *Hoxc9−/−* and *Hoxc9* ^{CM} mice labeled MNs restricted to segments C5-T1, similar to controls (Figure S3B), indicating ectopic LMC neurons are not rerouted to the limb. Because ectopic LMC neurons have been shown to target intercostal muscle in *Hoxc9* mutants (Jung et al., 2010), we assessed triceps pSN-thoracic LMC connectivity after injection of tracers into each of these muscle groups. This analysis revealed that thoracic LMC neurons target intercostal muscles and receive input from triceps pSNs (Figure S3C). In addition, the distribution of cervical SNs targeting triceps muscle was unaffected in *Hoxc9* mutants (Figure S3D), indicating the alterations in sensory-motor connectivity are not due to changes in the source of pSNs targeting the triceps.

We next assessed whether limb pSNs have the capacity to deliver sensory information to ectopic LMC neurons in *Hoxc9* mutants. We isolated spinal cords from *Hoxc9* mutants, stimulated C7 dorsal roots, and measured MN responses by ventral root recordings at segmental levels C7 and T3 (Figure S3E). In both control and *Hoxc9* mutants, after C7 dorsal root stimulation, C7 MNs exhibited short-latency monosynaptic responses followed by slower polysynaptic responses (Figure S3E). Onset latencies, monosynaptic response peak times, and peak amplitudes were not significantly different between control and *Hoxc9* mutants at C7 (Figure S3E). In contrast, in global *Hoxc9* mutants T3 ventral roots showed responses that were markedly increased in amplitude (0.40±0.05 mV in n=9 *Hoxc9−/−* mice vs. 0.05±0.01 mV in n=3 controls; **p=0.0015) (Figure 3D). Similarly, in *Hoxc9*^{CM} mice, upon C7 dorsal root stimulation, responses amplitudes at T3 were markedly increased (0.31 ±0.04 mV in n=4 *Hoxc9*^{CM} mice, versus 0.1±0.01 mV in n= 10 controls, ****p<0.0001) (Figure 3H). The increased T3 amplitudes in *Hoxc9* mutants likely reflect the presence of ectopic synapses from limb pSNs, but may also be due to changes in MN input resistance, as a consequence of their transformation to an LMC fate. Onset latencies at T3 were similar between control and *Hoxc9* mutants (Figure 3D,H), possibly due to the presence of some sensory projections to the thoracic MNs in controls. Collectively, these data indicate that cervical pSNs establish functional connections with ectopic LMC neurons in *Hoxc9* mutants.

In *Hoxc9* mutants the switch of MNs to an LMC fate is accompanied by a derepression of cervical *Hox* genes in both MNs and interneuron populations (Figure S2E). The alterations in pSN afferent connectivity could be solely due to changes in MNs, independent of changes of in interneurons, or dependent on programs acting within both populations. To address this, we assessed whether the changes in sensory-motor connectivity in *Hoxc9* mutants rely on the LMC determinant *Foxp1*, a transcription factor essential for LMC specification

(Dasen et al., 2008; Rousso et al., 2008). To remove both *Hoxc9* and *Foxp1* from MNs, we combined *Hoxc9 flox*, *Foxp1 flox*, and *Olig2::Cre* alleles. In $Hoxc9^{CM}$; $Foxp1^{CM}$ mice, no ectopic Raldh2^{+} MNs were detected at thoracic levels (Figure S2F). In contrast a *Hox* gene normally expressed at cervical levels, *Hoxc6*, was derepressed in thoracic MNs of both $Hoxc9^{CM}$;$Foxp1^{CM}$ and $Hoxc9^{CM}$ mice (Figure S2E). Combined removal of *Foxp1* and *Hoxc9* in MNs therefore prevents the generation of ectopic LMC neurons, but still leads to the derepression of cervical *Hox* genes (Figure S2G).

Cervical sensory afferents were traced by DiI injection into DRG C7 of $Hoxc9^{CM}$;$Foxp1^{CM}$ mice. Ventrally extending sensory afferents were not observed at thoracic levels after combined removal of *Hoxc9* and *Foxp1* (Figure 2A–C). Limb pSN afferents were also traced by CTB injection into the triceps muscle in double conditional mutants. No vGluT1^{+};CTB^{+} terminals were observed on thoracic MNs (Figure 2D). In addition the amplitudes of T3 ventral root recording after C7 dorsal root stimulation were similar between control, $Foxp1^{CM}$, and $Hoxc9^{CM}$;$Foxp1^{CM}$ mice (Figure S3F). These results indicate that the altered sensory-motor connectivity observed in *Hoxc9* mutants is due to activation of LMC programs within thoracic MNs.

MN Columnar Organization Determines Premotor Interneuron Input Pattern

Mutation in cell fate determinants can affect multiple features of MNs, including neuronal settling position and dendritic architecture (Surmeli et al., 2011; Vrieseling and Arber, 2006). In *Hoxc9* mutants, we found that transformed thoracic MNs were shifted to a more dorsolateral position, and their dendrites project radially, similar to cervical LMC neurons (Figure S4A–C). These changes in somatodendritic architecture could in principle affect MN connectivity with several premotor populations, including the diverse classes of spinal interneurons (INs) essential to coordinate MN firing.

Studies investigating the sources of spinal INs targeting MNs have revealed marked differences in the types and distribution of INs that synapse with specific columnar subtypes (Goetz et al., 2015). LMC neurons receive inputs from premotor INs that are positioned predominantly ipsilateral to the target limb. In contrast, thoracic HMC neurons receive inputs from INs that are distributed both contralaterally and ipsilaterally, with bias towards contralateral populations. To determine whether MN columnar identity has a role in shaping IN connectivity pattern, we examined premotor inputs in *Hoxc9* mutants. Because ectopic LMC neurons project to the normal muscle targets of thoracic HMC neurons (Jung et al., 2010), we assessed premotor INs that synapse with MNs targeting intercostal muscle.

Premotor interneurons were labeled via viral monosynaptic tracing methods (Stepien et al., 2010; Tripodi et al., 2011). Glycoprotein-deficient rabies virus expressing RFP protein (Rab-RFP) and adeno-associated virus expressing glycoprotein (AAV-G) were injected intramuscularly (Figure 4A). Viruses were injected into rostral intercostal muscles at P5 and the distribution of labeled premotor interneuron populations was examined at cervical and thoracic levels at P13. In controls, intercostal premotor INs were evenly distributed between the ipsilateral and contralateral side of injection (48% ipsilateral versus 52% contralateral at thoracic levels) (Figure 4B,C). In contrast, in global *Hoxc9* mutants, premotor INs were shifted towards an ipsilateral bias (70% ipsilateral versus 30% contralateral at thoracic

levels) (Figure 4B,C), a distribution similar to that of LMC premotor IN populations (Goetz et al., 2015). The ipsilateral shift in the distribution of labeled INs was observed at both thoracic and cervical levels, reflecting changes in the connectivity of both intrasegmental and descending premotor INs.

To determine whether the shift in premotor input distribution is specifically due to changes in MNs, we performed rabies tracing experiments in *Hoxc9*^{CM} mice. As with *Hoxc9* global mutants, after tracing from intercostal muscle there was a pronounced shift in premotor IN inputs to the ipsilateral side of the spinal cord (65% ipsilateral versus 35% contralateral at thoracic levels) (Figure 4B,C). Interestingly at thoracic levels there was a loss of a population of contralateral premotor INs in *Hoxc9* global mutants that were retained in *Hoxc9*^{CM} mice (Figure 4B), suggesting *Hoxc9* is also required in certain IN types for connectivity to MNs. These results indicate the columnar identity of MNs has a profound impact on determining the pattern of inputs from premotor IN populations (Figure 4D).

Discussion

Coordinate control of limb muscles depends on the specificity of connections established between MN subtypes and diverse classes of premotor neurons. While studies have shown that MNs can play an instructive role in defining functional properties of locomotor networks, the role of MN identity in spinal circuit assembly has remained unclear. We found that Hox-dependent programs in MNs are essential in shaping the patterns of connectivity between proprioceptive sensory neurons, spinal interneurons, and MN columnar subtypes. These findings indicate that MN identity plays a significant role in regulating premotor synaptic specificity in locomotor circuits.

During sensory-motor circuit assembly, proprioceptive sensory neurons synapse with MNs innervating the same muscle peripherally but avoid MNs projecting to functionally antagonistic muscles (Eccles et al., 1957; Frank and Mendelson, 1990). Studies on the mechanisms contributing to specificity in stretch-reflex circuits have largely focused on how pSNs select MN pools within a single segment (Mendelsohn et al., 2015; Surmeli et al., 2011; Vrieseling and Arber, 2006). However, in order to achieve correct wiring, pSNs must project over multiple segments to locate the position of their appropriate postsynaptic targets. Remarkably, a single pSN can establish highly selective connections with each of the ~50–200 MNs within a pool supplying a given limb muscle (Mendell and Henneman, 1968). Although sensory neurons are known to project long distances along the rostrocaudal axis, and extend ventrally to the position of MNs (Eide and Glover, 1995; Ozaki and Snider, 1997), the mechanisms through which they select postsynaptic targets over multiple segments are unknown.

We found that MN topographic organization determines the central termination of pSN axons within the ventral spinal cord. Transformation of thoracic HMC neurons to an LMC fate, through mutation of the *Hoxc9* gene, causes limb pSNs to extend to MNs at thoracic levels, where they establish functional connections with MNs. This alteration in connectivity does not appear to be a consequence of changes in MNs due to limb-derived signals, since ectopic LMC neurons in *Hoxc9* mutants project to hypaxial muscle. Analysis of a single

muscle target in *Hoxc9* mutants revealed that limb pSNs synapse and establish functional connections with thoracic LMC neurons. These results indicate that altered central connectivity of pSNs in *Hoxc9* mutants is due to changes in MN-intrinsic programs.

In addition to establishing connections with limb pSNs, LMC neurons synapse with multiple classes of spinal interneurons. Recent studies have shown that MNs can exert instructive roles in determining basic properties of locomotor circuits (Hinckley et al., 2015; Machado et al., 2015; Song et al., 2016), but whether MN identity determines connectivity with spinal interneurons has not been tested. We found that after global or conditional removal of *Hoxc9*, the distribution of intercostal premotor INs shifts to an ipsilateral bias, similar to patterns normally observed for limb MNs (Goetz et al., 2015). As with the alterations in sensory-motor connectivity in *Hoxc9* mutants, these changes do not appear to be due to peripheral signals provided by the limb, indicating MN-intrinsic programs regulate connectivity between spinal interneurons and columnar subtypes.

Several lines of evidence indicate that the changes in central connectivity observed in *Hoxc9* mutants are specifically due to transformation of MN columnar identities. We found that the rerouting of limb pSNs to ectopic LMC neurons in $Hoxc9^{CM}$ mice requires the LMC determinant *Foxp1*. After combined removal of both *Hoxc9* and *Foxp1* from MNs, cervical sensory afferents fail to synapse with thoracic MNs, similar to controls. Although we are unable to assess premotor IN connectivity in $Hoxc9^{CM}; Foxp1^{CM}$ mice, due to the lethality of this mutation, the majority of ipsilateral LMC premotor interneurons derive from an $Lbx1^{+}$ domain that is not targeted by *Olig2::Cre* excision. Since our rabies tracing strategy labels INs that are connected to MNs via a single synapse, the changes in premotor input distribution reflect the loss of *Hoxc9* from MNs.

How might Hox-dependent programs in MNs determine patterns of premotor connectivity? Given the diverse roles of Hox proteins in motor axon target selectivity, the central connectivity changes observed in *Hoxc9* mutants likely involve alterations in multiple downstream molecular pathways. In addition, we found that *Hoxc9* mutation alters the settling position and dendritic architecture of transformed MN populations. The alteration in premotor connectivity in *Hoxc9* mutants therefore could reflect changes in both the molecular and somatodendritic features of MNs. These results are consistent with the view that sensory-motor circuit assembly relies on both positional and molecular recognition cues (Jessell et al., 2011), and extend the influence of MN subtype identity to additional premotor neuronal classes.

Locomotion requires the coordinated activation of dozens of limb muscles, which requires more selective connections between MNs and premotor populations. While our study focuses on a single *Hox* gene and the role of columnar identity in spinal circuit connectivity, a similar logic could apply to pools of MNs targeting specific limb muscles. In addition, the same *Hox* genes expressed by LMC neurons are also present in interneurons and pSNs, suggesting that a common group of regulatory factors drives connectivity. The assembly of locomotor circuits may depend on a set of initial cues from MN columnar subtypes, which provide a broad set of instructions to premotor populations, operating in parallel with Hox-dependent programs in several neuronal classes.

Experimental Procedures

Mouse genetics

Animal work was approved by the Institutional Animal Care and Use Committee of the NYU School of Medicine (Protocol 160308) in accordance with NIH guidelines. Generation of floxed-*Hoxc9* mice and additional strains are described in Supplemental Experimental Procedures. No phenotypic differences between animals of different genders are expected, but were not formally tested.

DiI tracing

Animals were perfused with PBS and 4% PFA, and post-fixed for 2hr at 4C. ~3μl of DiI-ethanol solutions were applied to a slide glass to form a thin layer of DiI crystals. DiI crystals were injected into DRGs using a sharp tungsten needle. Injected tissue was incubated in 4% PFA for 10~30 days at 37°C. Spinal cords were vibratome sectioned at a thickness of 150μm.

CTB tracing

1~2% CTB (Sigma-Aldrich) solutions were injected into the triceps muscle at P3–4 and examined after 2 days. Pups were perfused with PBS and 4% PFA. Spinal cords were isolated and post-fixed for 2–6 hours at 4°C. Tissue was vibratome sectioned (at 100μm) or cryosectioned (at 30μm).

Extracellular recordings

Methods for ventral root recordings are described in Supplemental Experimental Procedures.

Viral tracing

Methods for viral tracing are described in Supplemental Experimental Procedures.

Immunohistochemistry

Primary antibodies against Hox proteins, Foxp1, Isl1/2, and Raldh2 have been described previously (Dasen et al., 2008; Dasen et al., 2005; Jung et al., 2010). Commercial antibodies included: nNos1 (rabbit, 1:10000, Immunostar), ChAT (goat, 1:200, Millipore), CTB (goat, 1:4000, List Biological Lab.; rabbit, 1:2000, Sigma-Aldrich), and vGluT1 (guinea pig, 1:1000, Millipore). Detailed protocols for histology are available on the Dasen lab website (http://www.med.nyu.edu/dasenlab/)

Imaging and image processing

A Zeiss Confocal Microscope (LSM700 with 20× dry or 63× oil objective lens) was used to acquire images. Images were processed in Fiji and Photoshop.

Statistics

Data were analyzed using GraphPad Prism6 software. Data are shown as averages ± SEM. Values were compared using Student's two-tailed t-test, and p values less than 0.05 were considered significant. Animal numbers are indicated in figures and legends.

Supplementary Material

Refer to Web version on PubMed Central for supplementary material.

Acknowledgments

We thank Helen Kim and David Lee for technical support, Anders Enjin, Michael Long, and George Mentis for advice with electrophysiology, and Polyxeni Philippidou and Richard Mann for feedback on the manuscript. This work was supported by NIH NINDS grants R01 NS062822 and R01 NS097550 to JD.

References

Arber S. Motor circuits in action: specification, connectivity, and function. Neuron. 2012; 74:975–989. [PubMed: 22726829]

Catela C, Shin MM, Dasen JS. Assembly and Function of Spinal Circuits for Motor Control. Annu Rev Cell Dev Bi. 2015; 31:669–698.

Chen JA, Huang YP, Mazzoni EO, Tan GC, Zavadil J, Wichterle H. Mir-17-3p controls spinal neural progenitor patterning by regulating Olig2/Irx3 cross-repressive loop. Neuron. 2011; 69:721–735. [PubMed: 21338882]

Dasen JS. Master or servant? emerging roles for motor neuron subtypes in the construction and evolution of locomotor circuits. Current opinion in neurobiology. 2016; 42:25–32. [PubMed: 27907815]

Dasen JS, De Camilli A, Wang B, Tucker PW, Jessell TM. Hox repertoires for motor neuron diversity and connectivity gated by a single accessory factor, FoxP1. Cell. 2008; 134:304–316. [PubMed: 18662545]

Dasen JS, Tice BC, Brenner-Morton S, Jessell TM. A Hox regulatory network establishes motor neuron pool identity and target-muscle connectivity. Cell. 2005; 123:477–491. [PubMed: 16269338]

Dessaud E, Yang LL, Hill K, Cox B, Ulloa F, Ribeiro A, Mynett A, Novitch BG, Briscoe J. Interpretation of the sonic hedgehog morphogen gradient by a temporal adaptation mechanism. Nature. 2007; 450:717–720. [PubMed: 18046410]

Eccles JC, Eccles RM, Lundberg A. The convergence of monosynaptic excitatory afferents on to many different species of alpha motoneurones. The Journal of physiology. 1957; 137:22–50.

Eide AL, Glover JC. Development of the longitudinal projection patterns of lumbar primary sensory afferents in the chicken embryo. The Journal of comparative neurology. 1995; 353:247–259. [PubMed: 7745134]

Frank E, Mendelson B. Specification of Synaptic Connections between Sensory and Motor Neurons in the Developing Spinal-Cord. J Neurobiol. 1990; 21:33–50. [PubMed: 2181066]

Goetz C, Pivetta C, Arber S. Distinct limb and trunk premotor circuits establish laterality in the spinal cord. Neuron. 2015; 85:131–144. [PubMed: 25543457]

Goulding M. Circuits controlling vertebrate locomotion: moving in a new direction. Nature reviews Neuroscience. 2009; 10:507–518. [PubMed: 19543221]

Grillner S. Biological pattern generation: the cellular and computational logic of networks in motion. Neuron. 2006; 52:751–766. [PubMed: 17145498]

Hinckley CA, Alaynick WA, Gallarda BW, Hayashi M, Hilde KL, Driscoll SP, Dekker JD, Tucker HO, Sharpee TO, Pfaff SL. Spinal Locomotor Circuits Develop Using Hierarchical Rules Based on Motorneuron Position and Identity. Neuron. 2015; 87:1008–1021. [PubMed: 26335645]

Jessell TM, Surmeli G, Kelly JS. Motor Neurons and the Sense of Place. Neuron. 2011; 72:419–424. [PubMed: 22078502]

Jung H, Lacombe J, Mazzoni EO, Liem KF Jr, Grinstein J, Mahony S, Mukhopadhyay D, Gifford DK, Young RA, Anderson KV, et al. Global control of motor neuron topography mediated by the repressive actions of a single hox gene. Neuron. 2010; 67:781–796. [PubMed: 20826310]

Livet J, Sigrist M, Stroebel S, De Paola V, Price SR, Henderson CE, Jessell TM, Arber S. ETS gene Pea3 controls the central position and terminal arborization of specific motor neuron pools. Neuron. 2002; 35:877–892. [PubMed: 12372283]

Luo LQ, O'Leary DDM. Axon retraction and degeneration in development and disease. Annual review of neuroscience. 2005; 28:127–156.

Machado TA, Pnevmatikakis E, Paninski L, Jessell TM, Miri A. Primacy of Flexor Locomotor Pattern Revealed by Ancestral Reversion of Motor Neuron Identity. Cell. 2015; 162:338–350. [PubMed: 26186188]

Mendell LM, Henneman E. Terminals of Single Ia Fibers - Distribution within a Pool of 300 Homonymous Motor Neurons. Science. 1968; 160:96-&. [PubMed: 4296007]

Mendelsohn AI, Simon CM, Abbott LF, Mentis GZ, Jessell TM. Activity Regulates the Incidence of Heteronymous Sensory-Motor Connections. Neuron. 2015; 87:111–123. [PubMed: 26094608]

Ozaki S, Snider WD. Initial trajectories of sensory axons toward laminar targets in the developing mouse spinal cord. The Journal of comparative neurology. 1997; 380:215–229. [PubMed: 9100133]

Pecho-Vrieseling E, Sigrist M, Yoshida Y, Jessell TM, Arber S. Specificity of sensory-motor connections encoded by Sema3e-Plxnd1 recognition. Nature. 2009; 459:842–846. [PubMed: 19421194]

Philippidou P, Dasen JS. Hox genes: choreographers in neural development, architects of circuit organization. Neuron. 2013; 80:12–34. [PubMed: 24094100]

Rossignol S, Dubuc R, Gossard JP. Dynamic sensorimotor interactions in locomotion. Physiological reviews. 2006; 86:89–154. [PubMed: 16371596]

Rousso DL, Gaber ZB, Wellik D, Morrisey EE, Novitch BG. Coordinated actions of the forkhead protein Foxp1 and Hox proteins in the columnar organization of spinal motor neurons. Neuron. 2008; 59:226–240. [PubMed: 18667151]

Song JR, Ampatzis K, Bjornfors ER, El Manira A. Motor neurons control locomotor circuit function retrogradely via gap junctions. Nature. 2016; 529:399-+. [PubMed: 26760208]

Stepien AE, Tripodi M, Arber S. Monosynaptic rabies virus reveals premotor network organization and synaptic specificity of cholinergic partition cells. Neuron. 2010; 68:456–472. [PubMed: 21040847]

Surmeli G, Akay T, Ippolito GC, Tucker PW, Jessell TM. Patterns of spinal sensory-motor connectivity prescribed by a dorsoventral positional template. Cell. 2011; 147:653–665. [PubMed: 22036571]

Tripodi M, Stepien AE, Arber S. Motor antagonism exposed by spatial segregation and timing of neurogenesis. Nature. 2011; 479:61–66. [PubMed: 22012263]

Vrieseling E, Arber S. Target-induced transcriptional control of dendritic patterning and connectivity in motor neurons by the ETS gene Pea3. Cell. 2006; 127:1439–1452. [PubMed: 17190606]

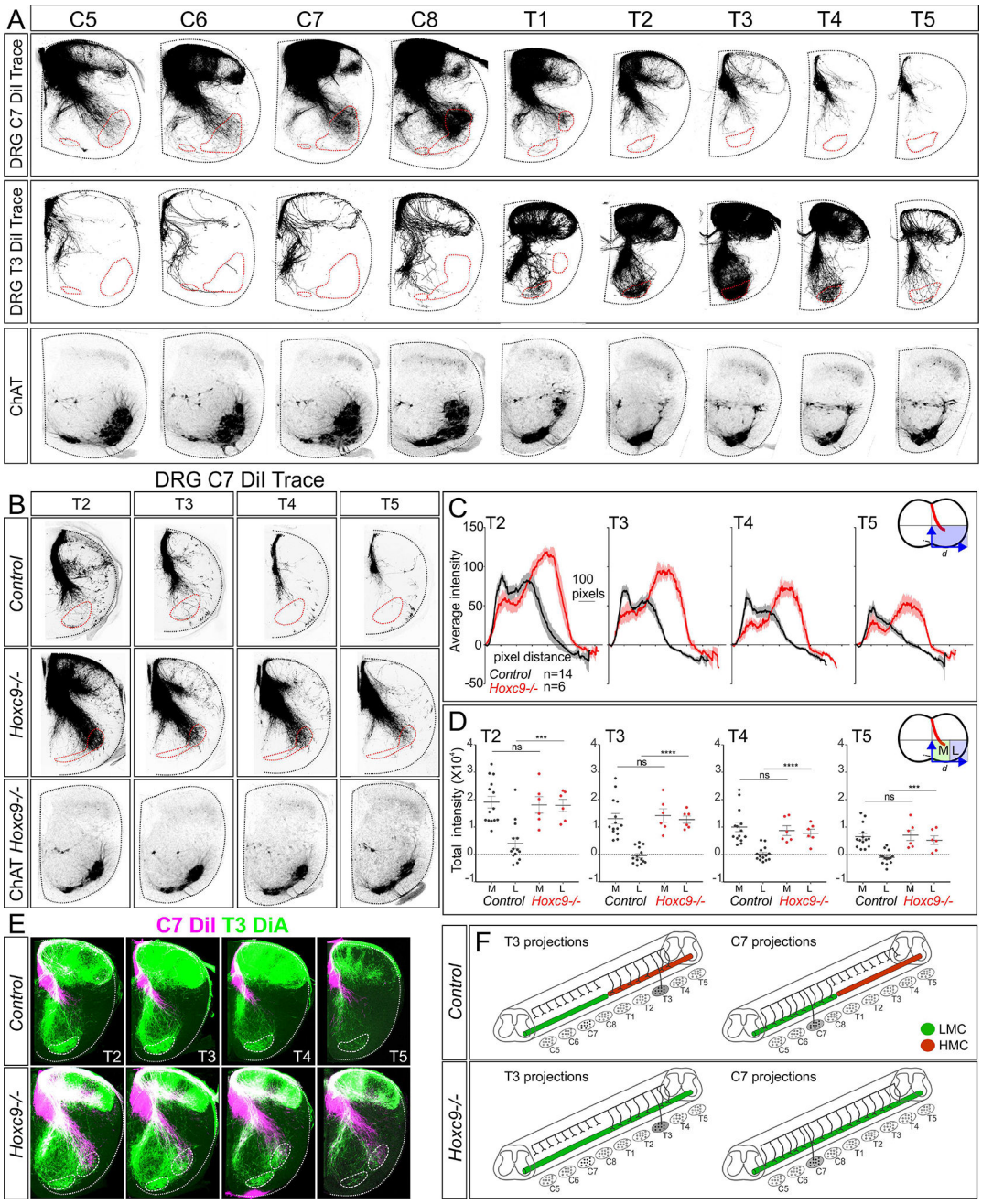

Figure 1. Hox-Dependent Programs Establish the Central Pattern of Sensory Projections

(A) Projections of SNs along the rostrocaudal axis of the spinal cord in control animals at P1. SNs were traced by DiI injection into DRG C7 and T3, and central projections were analyzed at indicated segments. Projections include a medial branch directed towards median motor column (MMC) neurons, and a lateral branch to non-MMC populations (LMC and HMC neurons). Bottom panels show choline acetyltransferase (ChAT) expression in MNs between segments C5–T5. (B) Projection of SNs to MNs in thoracic segments after DiI injections into DRG C7 in control and *Hoxc9−/−* mice at P0. Approximate MN position is outlined in red, based on ChAT. (C) Quantification of DiI pixel intensity along the

mediolateral axis in control and *Hoxc9−/−* mice. Lines show mean pixel intensity ±SEM from n=14 controls (E18.5, n=7; P0, n=7); and n=6 *Hoxc9−/−* mice (E18.5, n=4; P0, n=2), ***p=0.0007, T2; ****p<0.0001, T3; ****p<0.0001, T4; ***p=0.0003, T5. Inset shows region where distance (d) and pixel intensity (i) were measured. (D) Quantification of total DiI pixel intensity in medial and lateral regions of the spinal cord. In *Hoxc9* mutants there is an increase in lateral projections. (E) Comparison of C7 (DiI) and T3 (DiA) SN projections. Both C7 and T3 SNs project to MNs in *Hoxc9−/−* mice. (F) Summary of SN projections from T3 and C7 in control and *Hoxc9−/−* mice. See also Figure S1

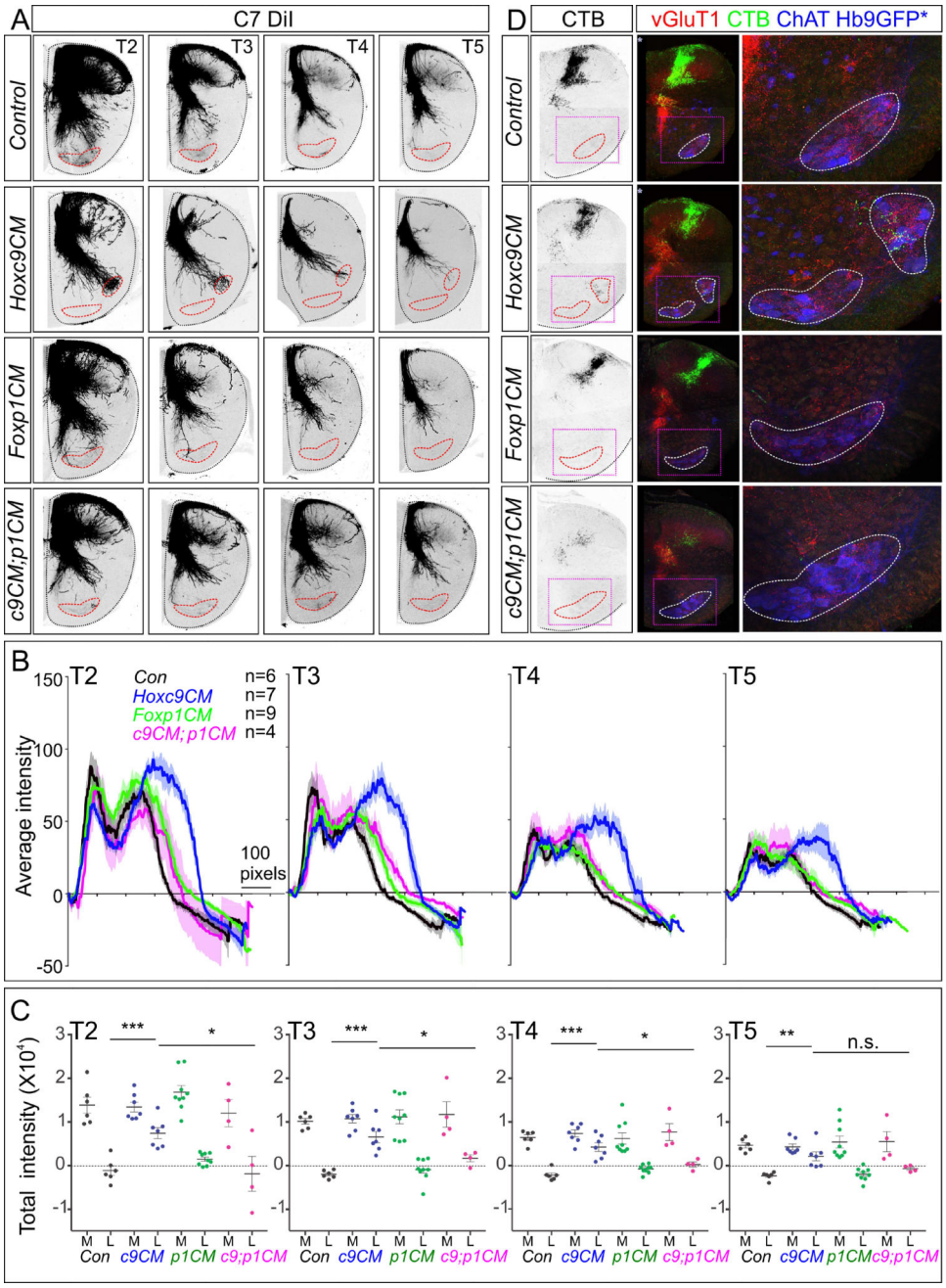

Figure 2. MN Columnar Identity Shapes Sensory-Motor Connectivity

(A) DiI tracing from DRG C7 analyzed at thoracic segments T2–T5 in indicated mouse mutants at P0. In *Hoxc9*^{CM}; *Foxp1*^{CM} double mutants and *Foxp1*^{CM} mice, SNs do not project to thoracic MNs. (B) Quantification of DiI traced DRG C7 sensory afferents in ventrolateral quadrant of segments T2–T5. Number of animals analyzed: Control, n=6 (P0, n=6); *Hoxc9*^{CM}, n=7 (P0, n=7); *Foxp1*^{CM}, n=9 (E18.5, n=3; P0, n=6); *Hoxc9*^{CM}; *Foxp1*^{CM}, n=4 (P0, n=4). (C) Quantification of total DiI pixel intensity in medial and lateral regions of the spinal cord. Pixel intensities in lateral position of *Hoxc9*^{CM}; *Foxp1*^{CM} and *Foxp1*^{CM} mice are similar to controls. ***p=0.0004, *p=0.0219, T2; ***p=0.0001, *p=0.0274, T3;

***p=0.0002, *p=0.0192, T4; **p=0.0025, ns=0.0747, T5. (D) Analysis of triceps sensory terminals in segment T3 at P5. In *Hoxc9*^{CM}; *Foxp1*^{CM} mice no CTB^{+} terminals are observed in the ventral spinal cord. n=3 each genotype. See also Figure S2.

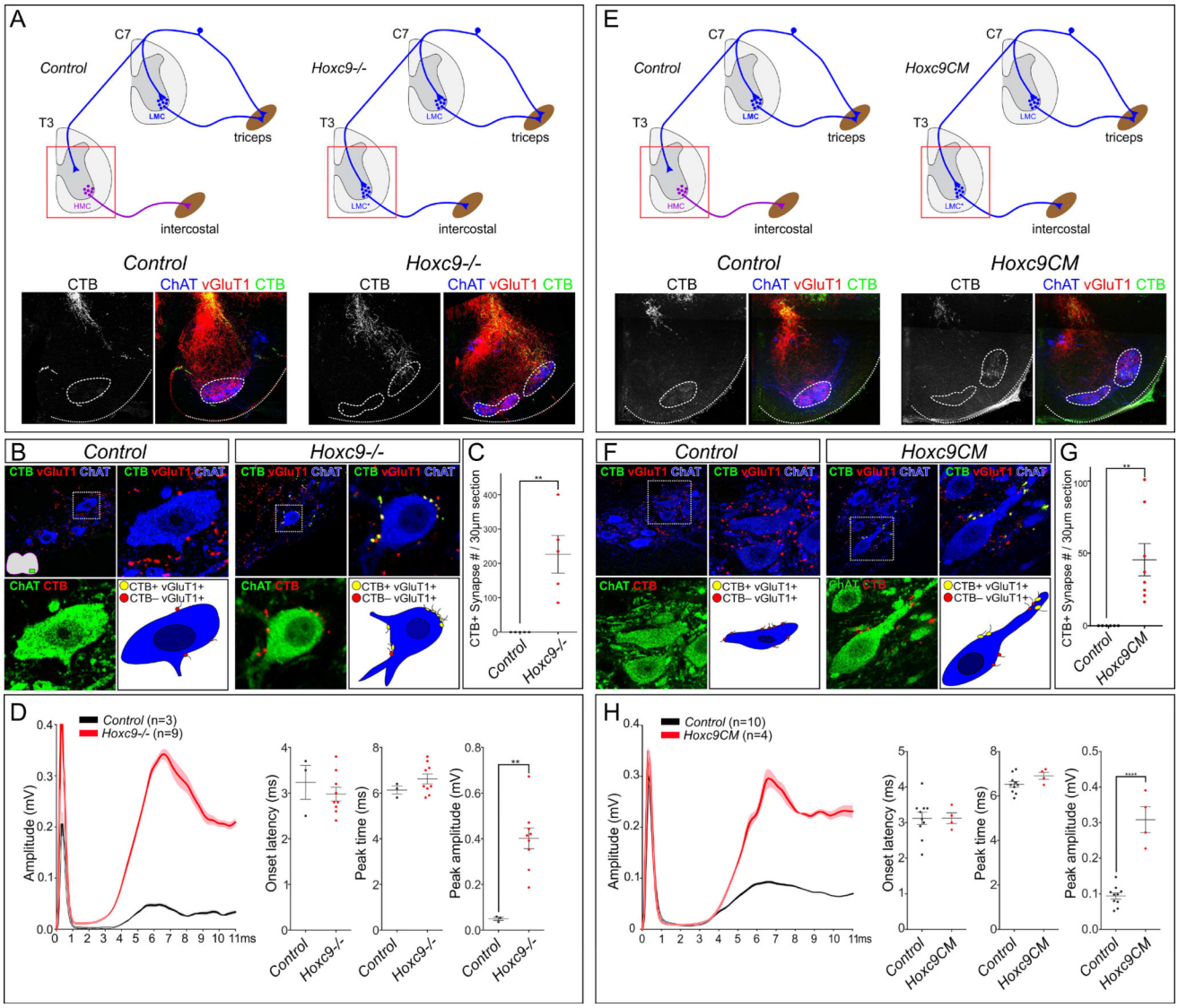

Figure 3. Limb pSNs Establish Synapses with Ectopic LMC Neurons in *Hoxc9* Mutants

(A) Localization of triceps pSN terminals in control and *Hoxc9−/−* mice at thoracic levels. Cervical pSN terminals were traced by injection of CTB into triceps muscles at P3 and examined at P5 at segment T3. (B) Triceps pSN terminals establish synapses on thoracic MNs in *Hoxc9−/−* mice. CTB^{+};$vGluT1^{+}$ are observed on MNs, marked by ChAT. (C) Quantification of CTB^{+} terminals on MNs at segment T3. Total synapses were counted in 30 μm sections. Controls, n=5, 0±0 (mean±SEM); *Hoxc9−/−* mice, n=5, 225.9± 54.44; **p=0.0032. (D) Quantification of onset latencies (control, 3.23±0.37 msec; *Hoxc9−/−*, 2.99±0.15 msec), peak time (control, 6.13±0.18 msec; *Hoxc9−/−*, 6.62±0.22 msec), and peak amplitude (control, 0.05±0.01 mV; *Hoxc9−/−*, 0.40±0.05 mV; **p=0.0015. Bars on graphs show mean ±SEM. (E) CTB tracing of triceps sensory terminals in thoracic segments of control and *Hoxc9*^{CM} mice. (F) Images of CTB traced triceps pSNs in thoracic segments. In *Hoxc9*^{CM} mice, CTB^{+};$vGluT1^{+}$ were observed on MNs. (G) Quantification of CTB^{+};$vGluT1^{+}$ terminals on thoracic MNs in control and *Hoxc9*^{CM} mice. Controls, n=6,

0±0 (mean ±SEM); *Hoxc9*^{CM}, n=8, 45.48±11.09. Bars, mean ±SEM; **p= 0.0043. (H) Traces of T3 ventral root signals upon C7 dorsal root stimulation in control (n=10) and *Hoxc9*^{CM} mice (n=4) at P6. Lines show mean ± SEM. Quantification of onset latencies (control, 3.12 ±0.17; *Hoxc9*^{CM}, 3.13 ±0.153), peak time (control, 6.52±0.13; *Hoxc9*^{CM}, 6.90±0.16), and peak amplitudes (control, 0.1±0.01; *Hoxc9*^{CM}, 0.31 ±0.04; ****p<0.0001). Bars show mean ±SEM. See also Figure S3.

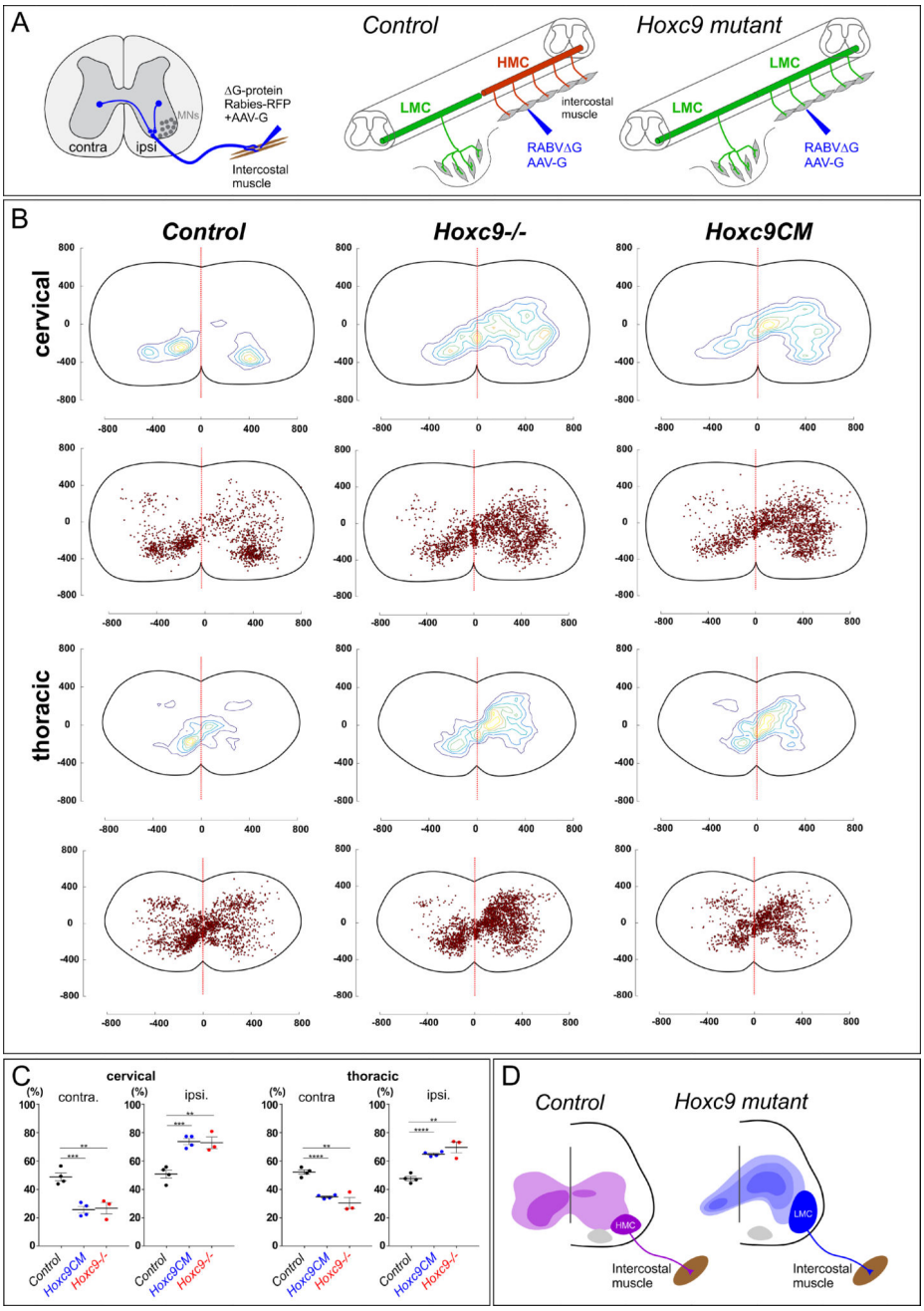

Figure 4. MN Columnar Identity Determines Premotor IN Input Pattern

(A) Schematic of viral tracing strategy. AAV-G and RABVΔG-RFP viruses were co-injected into rostral intercostal muscles at P5 and examined at P13. (B) Contour plots representing labeled premotor INs position. The regions with the greatest labeling density are encircled with yellow line. Red dotted line indicates midline of the spinal cord. Distances (μm) from the central canal are shown on X–Y axes. Cervical regions (C1–C8) and thoracic regions (T1–T13) are shown separately. Labeled cell position is shown beneath contour plots. Total number of labeled neurons: Control, n=4 mice, 1385 cells (cervical), 1895 (thoracic); *Hoxc9*^{CM}, n=4 mice, 1823 (cervical), 1412 (thoracic); *Hoxc9*−/−, n=3 mice, 2053 (cervical),

2325 (thoracic). (C) Quantification of ipsilateral vs. contralateral premotor populations at cervical and thoracic levels. Numbers represent averages from n=4 controls, n=4 *Hoxc9*^{CM} mice, and n=3 *Hoxc9*$^{-/-}$ mice. **p<0.001, ***p=0.0001, ****p<0.0001. Bar graphs show mean±SEM. (D) Summary of changes in premotor labeling in *Hoxc9* mutant mice. See also Figure S4.